Electronic Supplementary Information

Multi-Shelled CeO_2 Hollow Microspheres as Superior Photocatalysts for Water Oxidation

Jian Qi,[‡a] Kun Zhao,[‡ab] Guodong Li,[‡a] Yan Gao,[a] Huijun Zhao,[c] Ranbo Yu[*b] and Zhiyong Tang[*a]

Experimental Section

1. Reagents: The reagents including glucose, $CeCl_3 \cdot 7H_2O$, urea, hydrogen peroxide, sodium citrate, $FeCl_3 \cdot 6H_2O$, $CoCl_2 \cdot 6H_2O$, $NiCl_2 \cdot 6H_2O$, $CuCl_2 \cdot 2H_2O$, $ZnCl_2$, $CdCl_2$, $AgNO_3$ and commercial CeO_2 were all analytical grade in purity, and bought from Beijing Chemical Reagent Factory, Sinopharm Chemical Reagent Co., Ltd, Tianjin Jinke Fine Chemical Research Institute, Shantou Xilong Chemical Industry Incorporated Co., Ltd and Alfa Aesar, respectively. Ultrapure water (Millipore Milli-Q grade) with a resistivity of 18.2 MΩ was used in all the experiments.

2. Synthesis of multi-shelled CeO_2 hollow microspheres: In a typical procedure, 4.512 g urea was dissolved in 144 mL ultrapure water, and then 1.608 g $CeCl_3 \cdot 7H_2O$ was added, followed by stirred for 15 min to form a clear solution. Afterward, the above solution was added drop by drop into the 480 mL aqueous solution containing 43.2 g glucose. The mixture solution was subjected to vigorous stirring for 15 min to form a clear solution. Subsequently, the clear solution was transferred and sealed in the Teflon-sealed stainless steel autoclave. The autoclave was kept at 160 °C for 20 h. When the reaction was completed, the formed suspensions were deeply brown in color. A rinsing process including three cycles of washing procedure in ultrapure water was carried out before oven drying at 100 °C for 12 h. Finally, the solid powder was calcined in a muffle furnace under air atmosphere at 400 ^{o}C for 450 min, and the light yellow powder was obtained.

2.1 Synthesis of multi-shelled CeO_2 hollow microspheres with different amounts of glucose: Different amount of glucose (a: 0 g, b: 0.065 g, c: 0.129 g, d: 0.162 g, e: 0.324 g, f: 1.062g, g: 1.800 g, or h: 2.525 g) was dissolved into 20 mL ultrapure water to form a clear solution. Separately, 0.188 g urea was dissolved in 6 mL ultrapure water, and then 0.067 g $CeCl_3 \cdot 7H_2O$ was added, followed by stirred for 15 min to form a clear solution. Subsequently, the solution of urea and $CeCl_3$ was added drop by drop into the solution containing glucose under vigorous stirring for 15 min to form a clear mixture solution. After that, the mixture solution was transferred and sealed in the Teflon-sealed stainless steel autoclave and kept at 160 °C for 20 h. When the reaction was completed, the formed suspensions were deeply brown in color. A rinsing process including three cycles of washing procedure in ultrapure water was

carried out before oven drying at 100 °C for 12 h. Finally, the solid powders were calcined in a muffle furnace at 400 ^{o}C for 450 min under air atmosphere, and then the light yellow powders were obtained.

2.2 Synthesis of multi-shelled CeO_2 hollow submicrospheres with different amounts of urea: Different amount of urea (0 g, 0.094 g, 0.188 g, 0.376 g, 0.564 g and 0.752 g) was dissolved in 6 mL ultrapure water, and then 0.067 g $CeCl_3 \cdot 7H_2O$ was added, followed by stirred for 15 min to form a clear solution. Separately, 1.8 g glucose was dissolved in 20 mL ultrapure water to form a clear solution. The solution of urea and $CeCl_3$ was added drop by drop into the solution containing glucose under vigorous stirring for 15 min to form a clear solution. Afterward, the clear solution was transferred and sealed in the Teflon-sealed stainless steel autoclave and kept at 160 °C for 20 h. When the reaction was completed, the formed suspensions were deeply brown in color. A rinsing process including three cycles of washing procedure in ultrapure water was carried out before oven drying at 100 °C for 12 h. Finally, the solid powders were calcined in a muffle furnace at 400 ^{o}C for 450 min under air atmosphere, and then the light yellow powders were obtained.

2.3 Synthesis of multi-shelled CeO_2 hollow submicrospheres with different amounts of $CeCl_3 \cdot 7H_2O$: 1.8 g glucose was dissolved in 20 mL ultrapure water to form a clear solution. Separately, 0.188 g urea was dissolved in 6 mL ultrapure water, and then different amount of $CeCl_3 \cdot 7H_2O$ (0.0025 g, 0.0042 g, 0.0063 g, 0.0084 g, 0.0167 g, 0.0335 g, 0.067 g and 0.101 g) was added into the solution, followed by stirred for 15 min to form a clear solution. Subsequently, the solution of urea and $CeCl_3$ was added drop by drop into the solution containing glucose under vigorous stirring for 15 min to form a clear solution. After that, the clear solution was transferred and sealed in the Teflon-sealed stainless steel autoclave and kept at 160 °C for 20 h. When the reaction was completed, the formed suspensions were deeply brown in color. A rinsing process including three cycles of washing procedure in ultrapure water was carried out before oven drying at 100 °C for 12 h. Finally, the solid powders were calcined in a muffle furnace at 400 ^{o}C for 450 min under air atmosphere, and then the light yellow powders were obtained.

2.4 Synthesis of multi-shelled CeO_2 hollow submicrospheres at different crystallization temperatures: 0.752 g urea was dissolved in 24 mL ultrapure water, and then 0.268 g $CeCl_3 \cdot 7H_2O$ was added into the solution, followed by stirred for 15 min to form a clear solution. Afterward, the above solution was added drop by drop into 80 mL aqueous solution containing 7.2 g glucose to form a clear mixture solution. Subsequently, the mixture solution was divided into four parts, and then transferred and sealed in the Teflon-sealed stainless steel autoclave. The autoclave was kept at 110 °C, 140 °C, 160 °C and 180 °C for 20 h, respectively. When the reaction was completed, the formed suspensions were deeply brown in color. A rinsing process including three cycles of washing procedure in ultrapure water was carried out before oven drying at 100 °C for 12 h. Finally, the solid powders were calcined in a muffle furnace at 400 ^oC for 450 min under air atmosphere, and then the light yellow powders were obtained.

2.5 Synthesis of multi-shelled CeO_2 hollow submicrospheres at different crystallization time: 1.504 g urea was dissolved into 48 mL deionized water, and then 0.536 g $CeCl_3 \cdot 7H_2O$ was added, followed by stirred for 15 min to form a clear solution. Afterward, the above solution was added drop by drop into 160 mL aqueous solution containing 14.4 g glucose to form a clear mixture solution. Subsequently, the mixture solution was divided into eight parts, and then transferred and sealed in the Teflon-sealed stainless steel autoclaves. The autoclaves were heated at 160 °C for 1 h, 2 h, 4 h, 8 h, 10 h, 16 h, 20 h and 24 h, respectively. When the reaction was completed, the formed suspensions were deeply brown in color. A rinsing process including three cycles of washing procedure in ultrapure water was carried out before oven drying at 100 °C for 12 h. Finally, the solid powders were calcined in a muffle furnace at 400 ^oC for 450 min under air atmosphere, and then the light yellow powders were obtained.

3. Synthesis of multi-shelled M_xO_y hollow submicrospheres: In a typical synthesis procedure, 0.188 g urea was dissolved in 6 mL ultrapure water, and then $MCl_m \cdot nH_2O$ (1.78×10^{-4} mol, $FeCl_3 \cdot 6H_2O$, $CoCl_2 \cdot 6H_2O$, $NiCl_2 \cdot 6H_2O$, $CuCl_2 \cdot 2H_2O$, $ZnCl_2$, and $CdCl_2$, m=1~3, n=0~6) was added into the solution to form a clear solution. Afterward, the above solution was added drop by drop into 20 mL aqueous solution containing 1.8 g glucose to form a clear mixture solution. Subsequently, the mixture

solution was transferred and sealed in the Teflon-sealed stainless steel autoclave and kept at 160 °C for 20 h. When the reaction was completed, the formed suspensions were deeply brown in color. A rinsing process including three cycles of washing procedure in ultrapure water was carried out before oven drying at 100 °C for 12 h. Finally, the solid powders were calcined in a muffle furnace at 400 ^{o}C for 450 min under air atmosphere.

4. Synthesis of single-shelled CeO_2 hollow microspheres: In a typical synthesis procedure, 1.08 g urea was dissolved in 171 mL ultrapure water to form a clear solution, and then 72 mL sodium citrate solution (10 mM) was added into the above solution under vigorous stirring for 10 min. Subsequently, 0.89 g $CeCl_3 \cdot 7H_2O$ was added into the above solution, and the resulting mixture was kept for 15 min under stirring. After that, 1.08 mL hydrogen peroxide (30%) was added into the above-mentioned solution drop by drop under vigorous stirring for 30 min. Finally, the mixture was transferred to Teflon-lined stainless steel autoclaves and kept at 180 °C for 22 h. The resultant solid products were centrifuged, washed three times with distilled water, and dried at 100 °C in air atmosphere for 12 h. Finally, the light yellow powders were obtained.

5. Synthesis of double-shelled CeO_2 hollow microspheres: The double-shelled CeO_2 hollow microspheres were prepared according the reported literature with minor modification.[1] In a typical synthesis procedure, 1.0 g $Ce(NO_3)_3 \cdot 6H_2O$ was added to 40 mL mixed solution containing PEG-400 and H_2O with the volume ratio of 3:1 under vigorous stirring over 1 h in a flask. Subsequently, the reaction mixture was transferred into a 50 mL Teflon-lined stainless-steel autoclave and kept at 180 ^{o}C for 24 h. After that, the milky white precipitates were collected by washing several times with ultrapure water and ethanol, followed by drying in air at 80 ^{o}C for 5 h. Finally, the obtained products were subjected to the thermal treatment at 500 ^{o}C for 4 h to remove the organic template in the product.

6. Photocatalytic test: The photocatalytic experiments were carried out in a 300 mL pyrex reactor equipped with a Quartz lid under the photoirradiation conditions coupled with a gas chromatograph (Tianmei GC-7900) equipped with a thermal conductivity detector. 100 mg photocatalyst was dispersed in 100 mL $AgNO_3$ aqueous

solution and then stirred for 10 min. Subsequently, the suspensions were transferred into the reactor and purged by a vacuum pump before photoirradiation in order to remove the dissolved air. A 300 W xenon lamp with cutoff filiter (250 nm＜λ＜380 nm) (PLS-SXE300UV, Beijing Perfect Light Company) was used to irradiate the suspension, and the oxygen evolution was determined quantitatively by gas chromatography (GC).

7. Characterization: Powder XRD patterns were recorded on a Panaltical X'Pert-pro MPD X-ray power diffractometer using Cu Kα radiation (λ=1.54056 Å). SEM was performed on a Hitachi S-4800 electron microscope. TEM was performed on FEI Tecnai G^2 F20 electron microscope operated at 200 kV with the software package for automated electron tomography. FT-IR spectra (PE2000) were acquired to identify the structural vibration and surface functional groups of samples. Brunauer-Emmett-Teller (BET) surface area, pore volume and pore size of photocatalysts were measured using a Quadrasorb SI-MP instrument. Prior to each measurement, the samples were heated to 300 °C and kept for 3 h. XPS spectra were recorded by an ESCALAB 250 Xi XPS system of Thermo Scientific, where the analysis chamber was 1.5×10^{-9} mbar and the X-ray spot was 500 μm. UV-Vis diffuse reflection absorption spectra of the samples were obtained by an UV-Vis spectrometer (Lambda 950, PE, USA) equipped with an integrating sphere accessory in the diffuse reflectance mode (R) and $BaSO_4$ as a reference material.

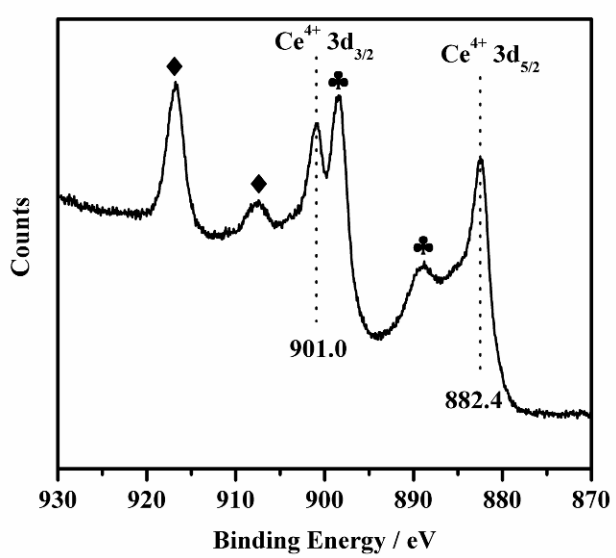

Fig. S1 Ce 3d XPS spectrum of TSCeHSs. The symbols ♦ and ♣ are the shake-up peaks of 901.0 eV and 882.4 eV, respectively.

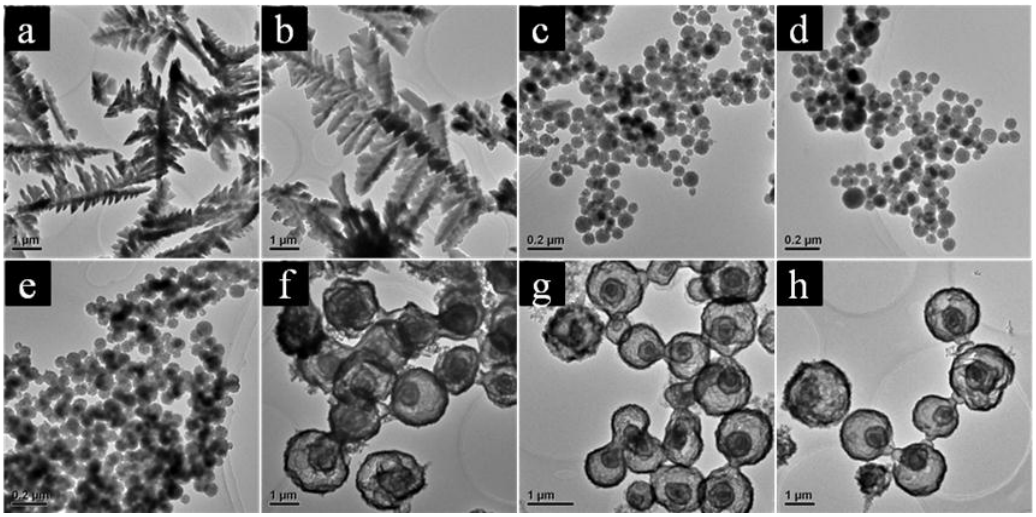

Fig. S2 TEM images of the samples obtained with different amounts of glucose in the solution containing $CeCl_3$ and urea at 160 °C for 20 h. a: 0 g, b: 0.065 g, c: 0.129 g, d: 0.162 g, e: 0.324 g, f: 1.062g, g: 1.800 g, and h: 2.525 g.

With increasing the amount of glucose from zero to a high amount, the morphologies of the products obtained are dendritic, solid spherical and triple-shelled hollow spherical structures in sequence, indicating that glucose acts as an important role in determining the morphology of final products.

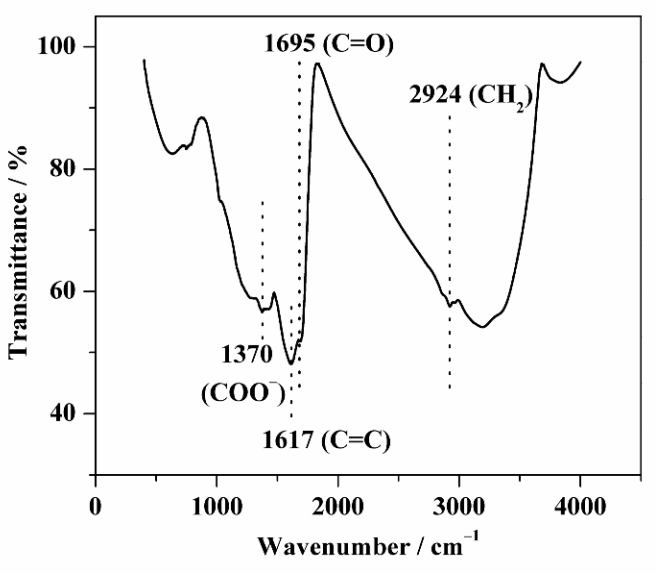

Fig. S3 FT-IR spectrum of pre-TSCeHSs.

The absorption bands at 1695 and 1617 cm^{-1} are assigned to C=O and C=C vibrations, indicating aromatization of glucose. The appearance of the COO^- absorption band at 1370 cm^{-1} mainly originates from carbonization of glucose. The bands in the range of 1000-1300 cm^{-1} include the C-OH stretching and OH bending vibrations, suggestive of existence of the residual hydroxy groups.

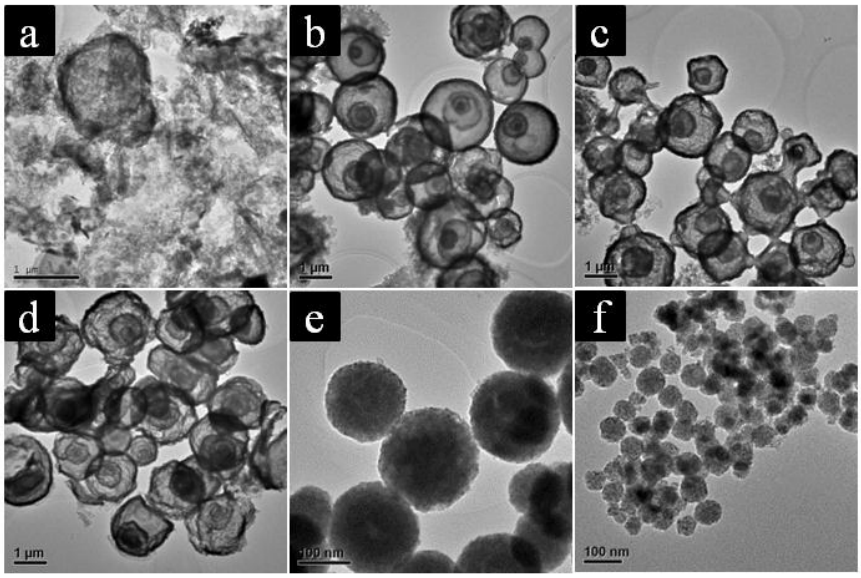

Fig. S4 TEM images of the samples obtained with different amounts of urea in the solution containing $CeCl_3$ and glucose at 160 °C for 20 h. a: 0 g, b: 0.094 g, c: 0.188 g, d: 0.376 g, e: 0.564 g and f: 0.752 g.

In the absence of urea, irregular particles are formed. With increasing the amount of urea, the morphologies of the products are triple-shelled hollow spheres and solid spheres in sequence. Decomposition would release OH^- ions, which promote the deprotonation of the functional groups inside the carbon microspheres and simultaneous formation of COO^- ions. When more COO^- ions are formed, more Ce^{3+} ions could be adsorbed through the electrostatic attractions, leading to transformation from hollow to solid spherical CeO_2.

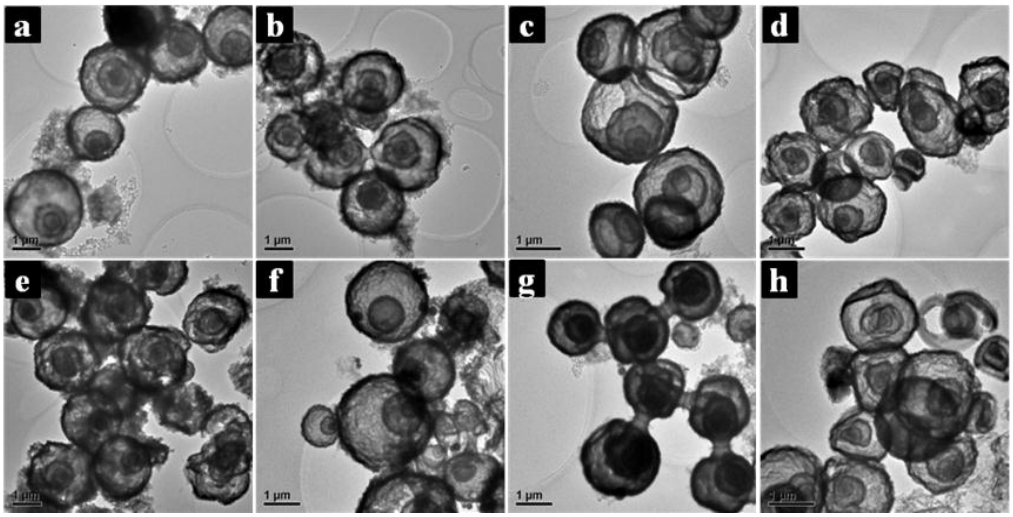

Fig. S5 TEM images of the samples obtained with different amounts of $CeCl_3$ in the solution containing glucose and urea at 160 °C for 20 h. a: 0.0025 g, b: 0.0042 g, c: 0.0063 g, d: 0.0084 g, e: 0.0167 g, f: 0.0335 g, g: 0.067 g and h: 0.101 g.

$CeCl_3$ has little effect on formation of TSCeHSs under the hydrothermal conditions used.

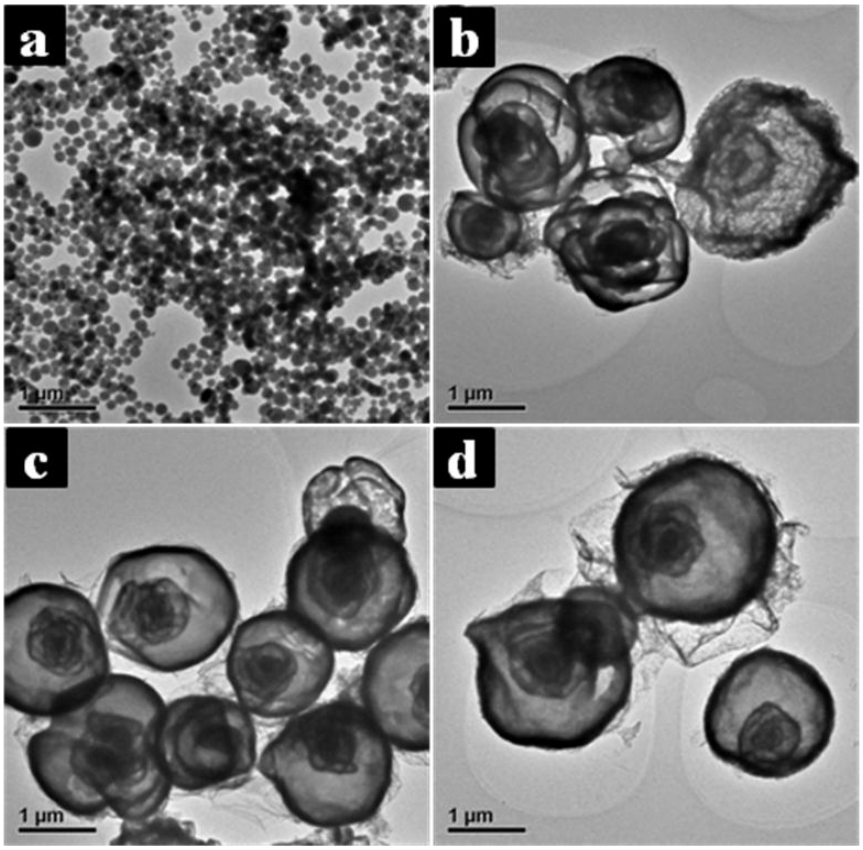

Fig. S6 TEM images of the samples obtained in the mixture solution containing $CeCl_3$, glucose and urea at different crystallization temperatures: (a) 110 °C, (b) 140 °C, (c) 160 °C and (d) 180 °C for 20 h.

At the lower crystallization temperature of 110 °C, smaller sized products are obtained and no multi-shelled hollow products are discerned. With increasing the crystallization temperature, only triple-shelled hollow microspheres of similar sizes are obtained.

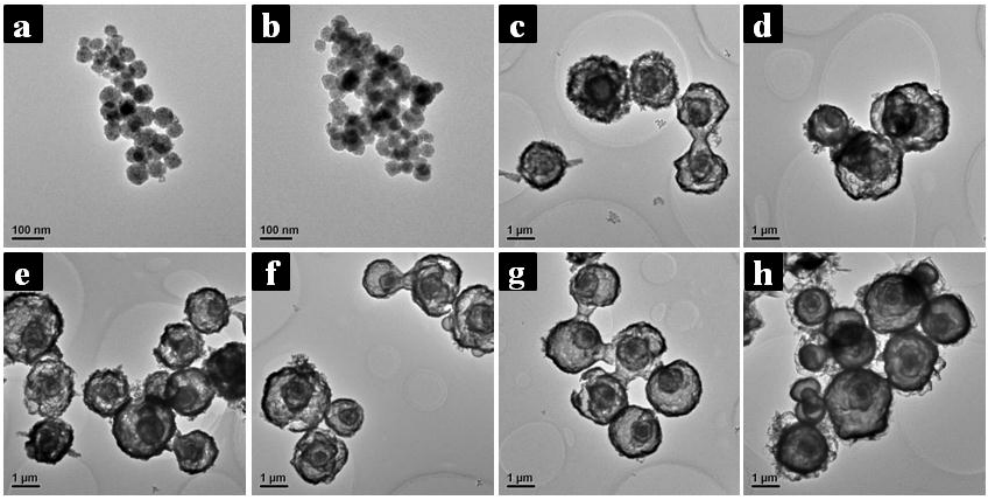

Fig. S7 TEM images of the samples obtained in the mixed aqueous solution containing $CeCl_3$, glucose and urea at 160 ^oC at different crystallization time: (a) 1 h, (b) 2 h, (c) 4 h, (d) 8 h, (e) 10 h, (f) 16 h, (g) 20 h and (h) 24 h.

At the reaction time of 1 h and 2 h, smaller sized products are obtained and no multi-shelled hollow products are discerned. With increasing the crystallization time, only triple-shelled hollow microspheres are obtained.

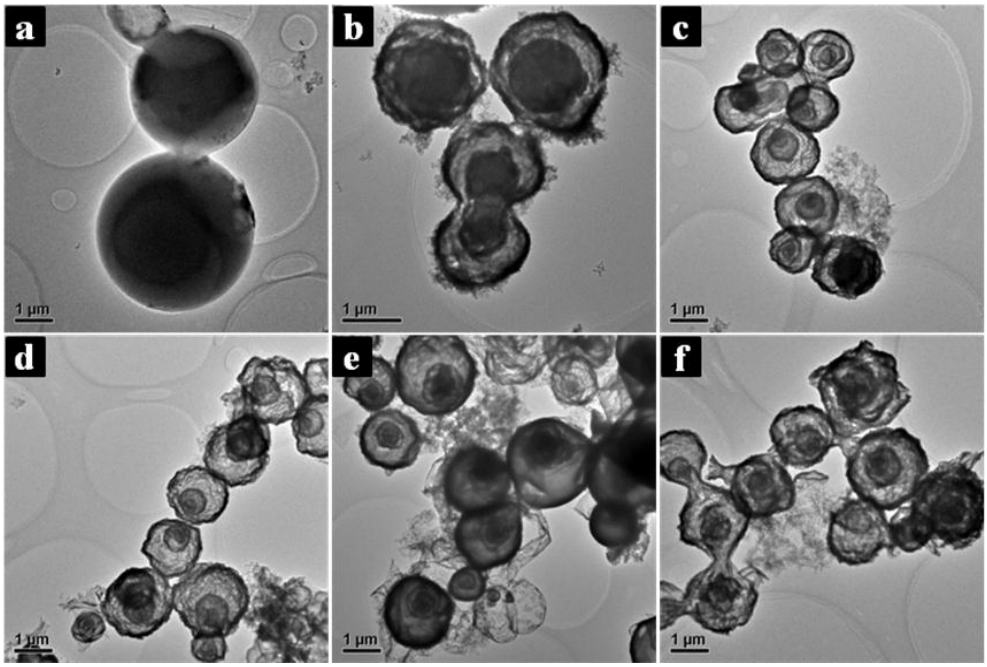

Fig. S8 TEM images of the samples obtained in the mixture solution containing $CeCl_3$, glucose and urea at 160 ^{o}C for 20 h subjected to different calcination temperatures: (a) 300 ^{o}C, (b) 350 ^{o}C, (c) 400 ^{o}C, (d) 450 ^{o}C, (e) 500 ^{o}C and (f) 550 ^{o}C for 30 min.

At the calcination temperature of 300 ^{o}C, the carbon source in the microspheres can not be removed, and the solid spherical products are obtained. With increasing the calcination temperatures, the carbon source is removed completely and only triple-shelled hollow microspheres of similar sizes are obtained.

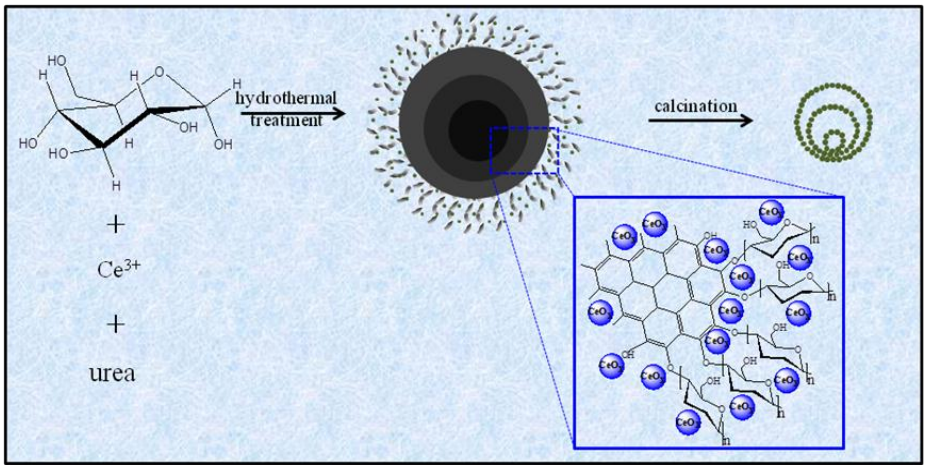

Fig. S9 Scheme of TSCeHSs formation process.

Firstly, the condensation and polymerization of glucose in the solution under hydrothermal conditions could contribute to formation of carbon microspheres. Subsequently, the functional groups of carbon microspheres are deprotonated in the alkaline environment from decomposition of urea, and Ce^{3+} ions are adsorbed through electrostatic attractions. After that, the spontaneously formed carbon microspheres are used as the sacrificial templates to generate TSCeHSs through calcination in air. We also notice that it is hard to achieve the CeO_2 hollow microspheres with single shell and double shells under the experimental conditions used, likely owing to the difficulty in controlling the nucleation and growth rate of cerium-based compounds in the carbon matrices under the hydrothermal conditions used.

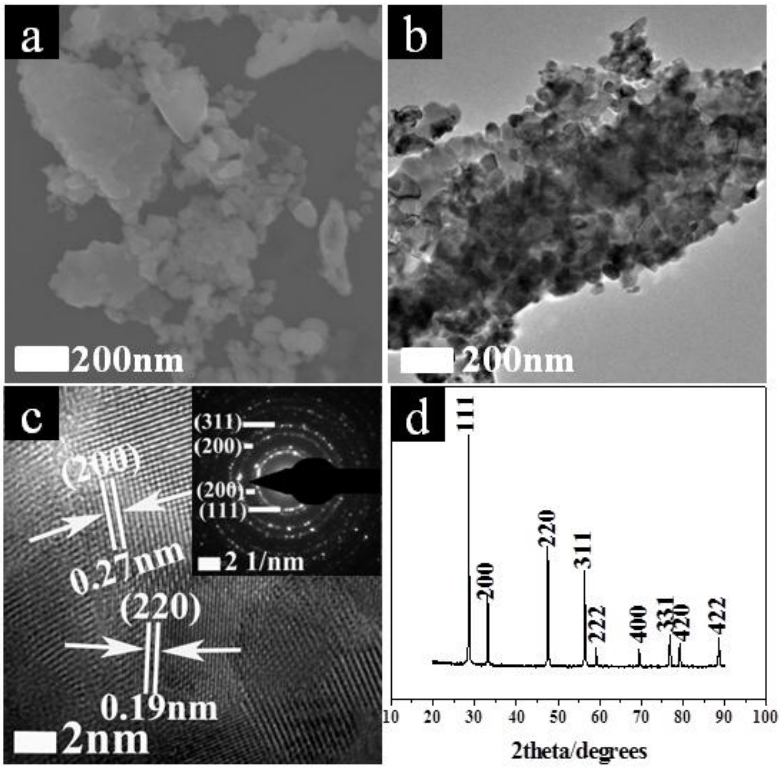

Fig. S10 (a) SEM image of commercial CeO_2 NPs. (b) TEM image of commercial CeO_2 NPs. (c) HRTEM image of the commercial CeO_2 NPs. Inset is selected area electron diffraction (SAED) image, indicating polycrystalline nature of the CeO_2 NPs. (d) XRD pattern of the commercial CeO_2 NPs. The commercial CeO_2 samples are sheet-like and composed by CeO_2 NPs of about 20-30 nm in diameter.

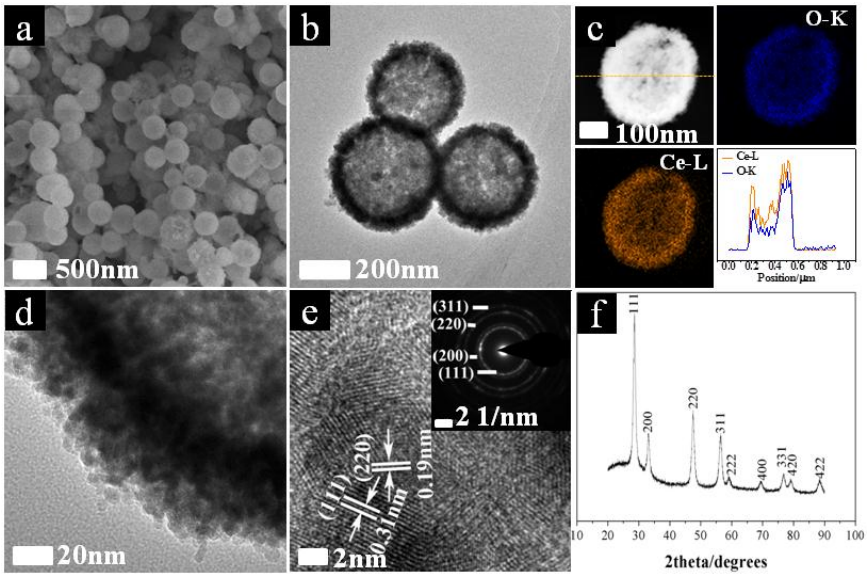

Fig. S11 (a) SEM image of SSCeHSs. (b) TEM image of SSCeHSs. (c) HAADF-STEM mapping image of the submicrosphere and the corresponding line-scan profiles. (d) TEM image of the CeO_2 shells. (e) HRTEM image of the submicrospheres. Inset is selected area electron diffraction (SAED) image, indicating polycrystalline nature of the CeO_2 shell. (f) XRD pattern of the submicrospheres. SSCeHSs are 300-400 nm in diameter and composed by CeO_2 NPs of about 6-13 nm in diameter.

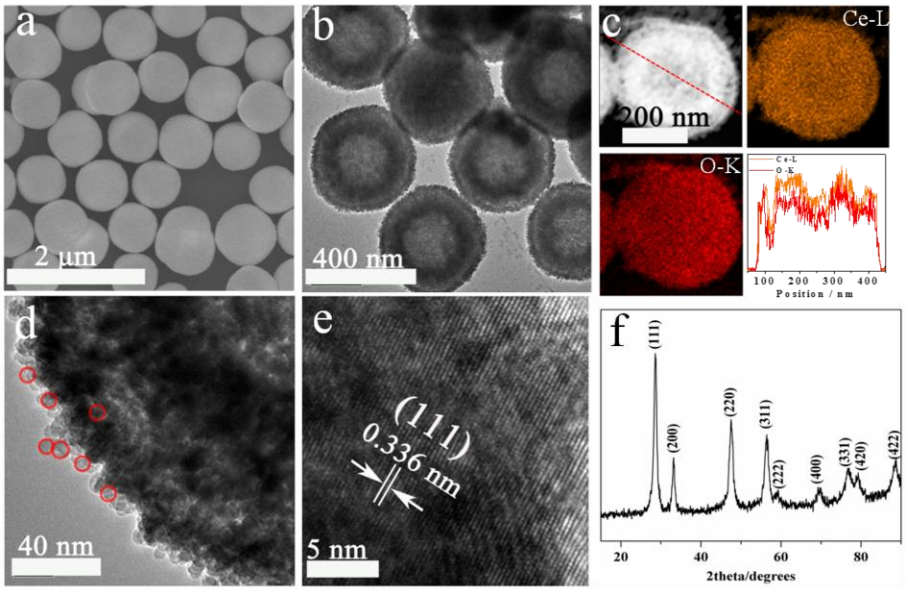

Fig. S12 (a) SEM image of DSCeHSs. (b) TEM image of DSCeHSs. (c) HAADF-STEM mapping image of the submicrosphere and the corresponding line-scan profiles. (d) TEM image of the CeO_2 shells. (e) HRTEM image of the submicrospheres. (f) XRD pattern of the submicrospheres. DSCeHSs are about 350-450 nm in diameter and composed by CeO_2 NPs of about 5-8 nm in diameter.

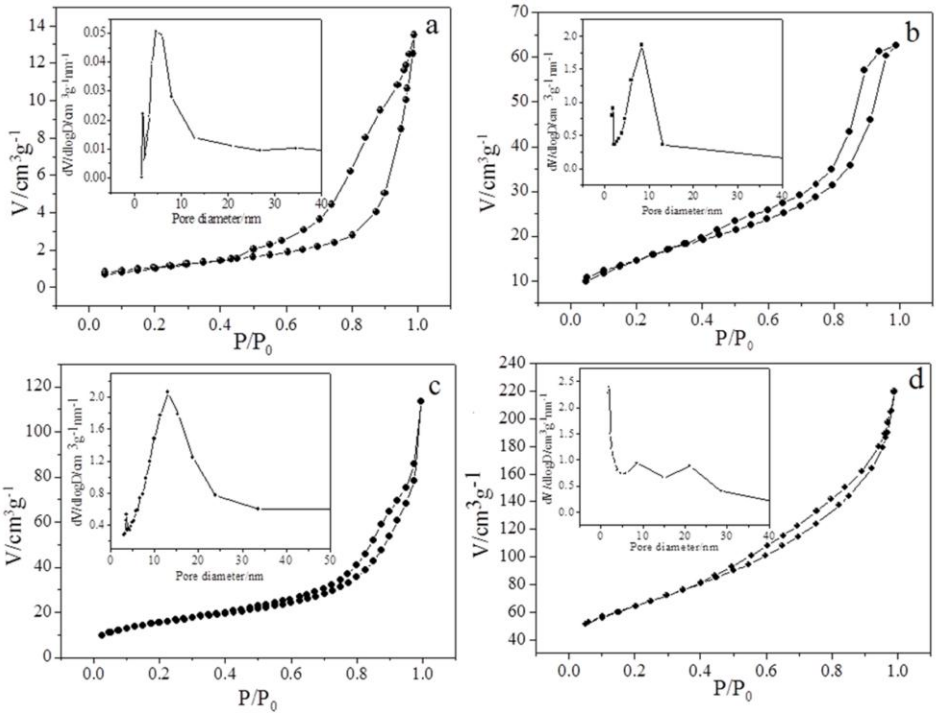

Fig. S13 N_2 adsorption-desorption isotherms and their corresponding pore-size distribution curves (inset) of (a) commercial CeO_2 NPs, (b) SSCeHSs, (c) DSCeHSs and (d) TSCeHSs.

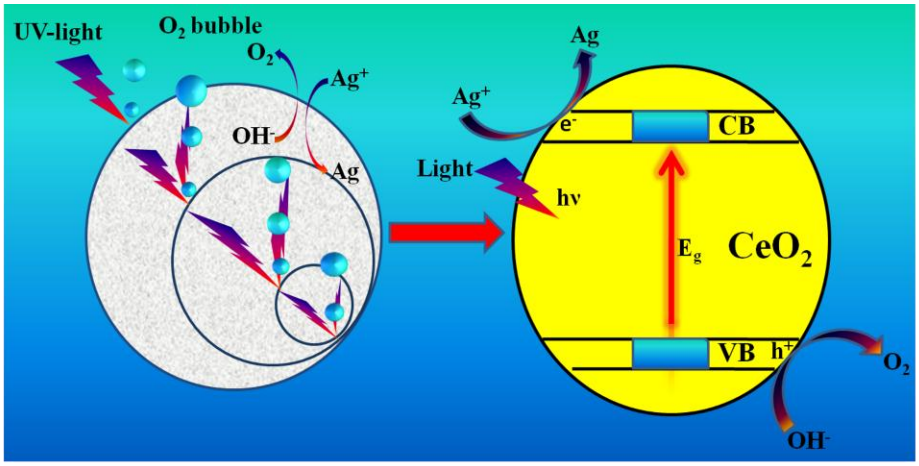

Fig. S14 Scheme of photocatalytic water oxidation over TSCeHSs with $AgNO_3$ as the electron scavenger under the photoirradiation.

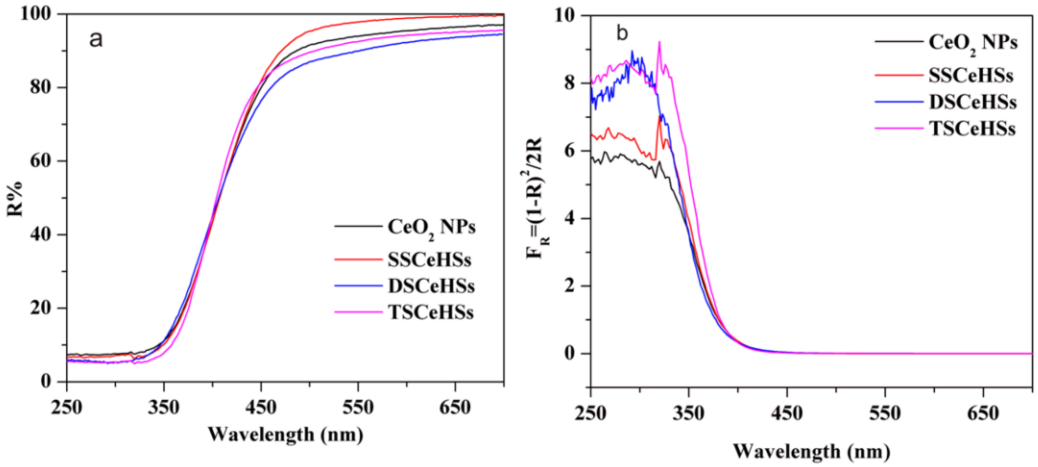

Fig. S15 (a) UV-Vis diffuse-reflectance spectra, and (b) corresponding Kubelka Munk function of the reflectance of commercial CeO_2 NPs, SSCeHSs, DSCeHSs and TSCeHSs.

It is observed from Figure S15b that Kubelka Munk Function becomes higher with the number interior compartments, suggesting that more photogenerated electron and hole pairs could be excited in TSCeHSs under the same UV irradiation condition.

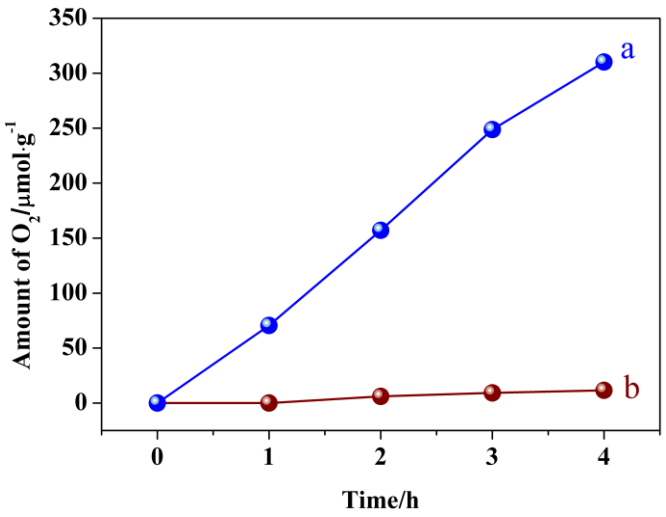

Fig. S16 O_2 evolution as a function of reaction time in 0.01 M $AgNO_3$ aqueous solutions under the photoirradiation: (a) with TSCeHSs, (b) without TSCeHSs.

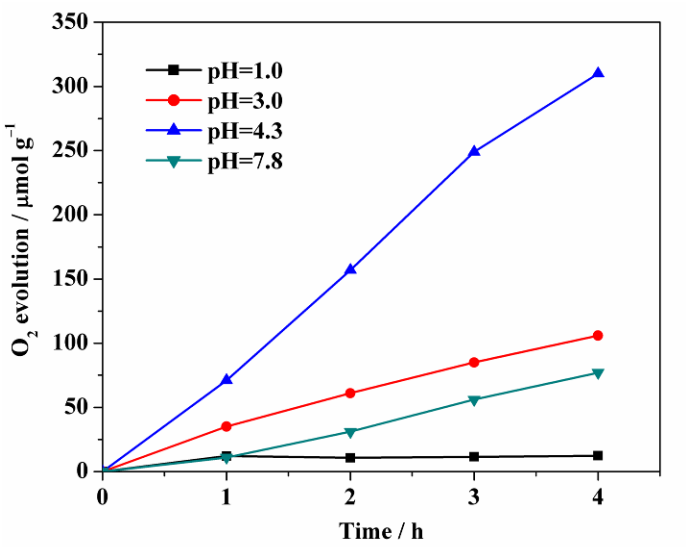

Fig. S17 Effect of different pH values on O_2 evolution in 0.01 M $AgNO_3$ aqueous solutions under the photoirradiation.

When the initial pH value of the solution is decreased from 4.3 to 1.0, the O_2 evolution is dropped to 4% of its initial value, suggesting that water oxidation preferably proceeds at higher pH value, which is similar to previous report that the formed O_2 can capture conduction band electrons to form $O_2^{\bullet-}$ radical and then react with H^+ ion to produce $H_2O^{\bullet}$, causing a decrease in O_2 evolution rate. When the initial pH value is further increased from 4.3 to 7.8, the O_2 evolution is dropped to 25% of its initial value. This may be attributed to the fact that Ag^+ ions are hydrolyzed into precipitate by OH^- ions at high pH values, thus lowering the concentration of Ag^+ ions and decreasing the capture rate of photogenerated electrons.

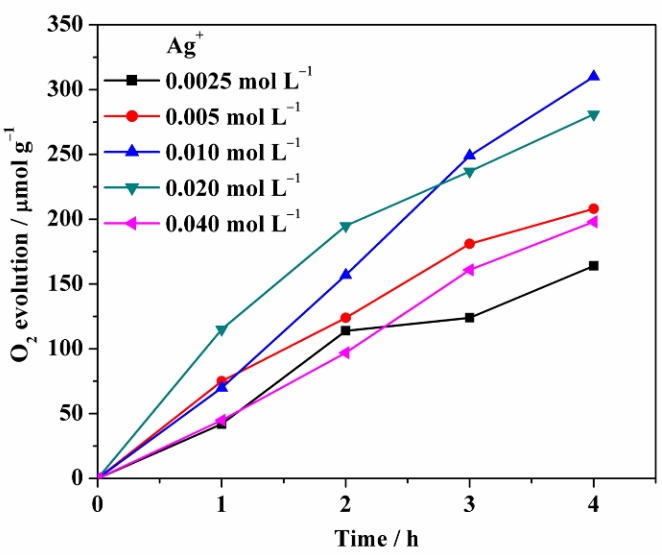

Fig. S18 Effect of different concentration of Ag^+ ions on O_2 evolution under the photoirradiation.

When the concentration of $AgNO_3$ aqueous solution is decreased from 0.01 M to 0.0025 M, the O_2 evolution is dropped to 53% of its initial value. However, when the concentration of $AgNO_3$ aqueous solution is increased from 0.01 M to 0.04 M, the O_2 evolution is also dropped to 64% of its initial value. This can be ascribed to the fact that higher concentration of $AgNO_3$ aqueous solution may promote the hydrolysis of Ag^+ ions to form precipitate, which deposits on the surfaces of the TSCeHSs and covers the active sites, thus leading to decrease of the O_2 evolution rate.

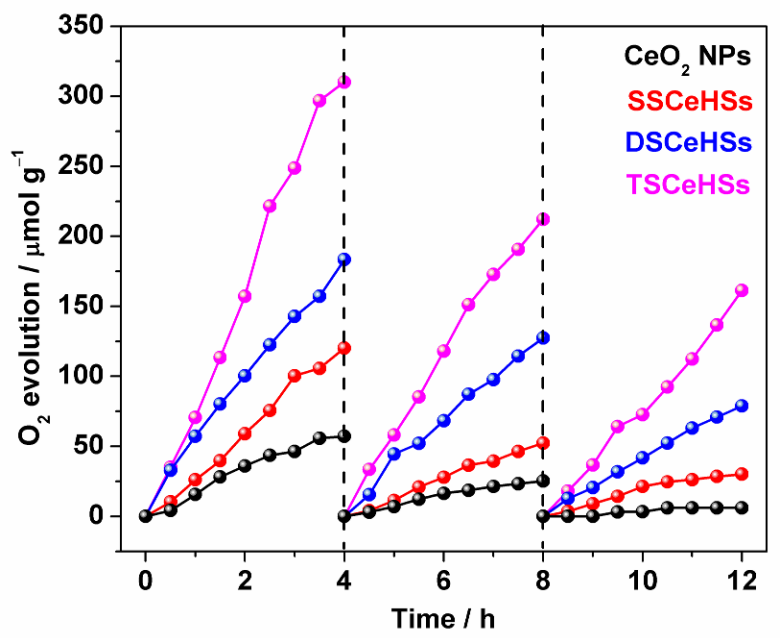

Fig. S19 Stability test of four photocatalysts including commercial CeO_2 NPs, SSCeHSs, DSCeHSs and TSCeHSs for direct water oxidation in 0.01 M $AgNO_3$ aqueous solution under the UV-light irradiation (250 nm $<$ λ $<$ 380 nm) by a series of repeated purge and injection cycles with an interval of 4 h.

With increasing the cycle number, the photocatalytic stability shows a gradual decrease, and the average O_2 evolution rates are decreased from 14 μmol g^{-1}_{cat} h^{-1} at the 1st cycle to 2 μmol g^{-1}_{cat} h^{-1} at the 3rd cycle for the commercial CeO_2 NPs, from 30 μmol g^{-1}_{cat} h^{-1} at the 1st cycle to 10 μmol g^{-1}_{cat} h^{-1} at the 3rd cycle for the SSCeHSs, from 46 μmol g^{-1}_{cat} h^{-1} at the 1st cycle to 20 μmol g^{-1}_{cat} h^{-1} at the 3rd cycle for the DSCeHSs, and from 78 μmol g^{-1}_{cat} h^{-1} at the 1st cycle to 40 μmol g^{-1}_{cat} h^{-1} at the 3rd cycle for the TSCeHSs, respectively. Correspondingly, the average O_2 evolution rates are dropped to 14.3%, 33.3%, 43.5% and 51.3% of the initial values for the commercial CeO_2 NPs, the SSCeHSs, the DSCeHSs and the TSCeHSs, respectively.

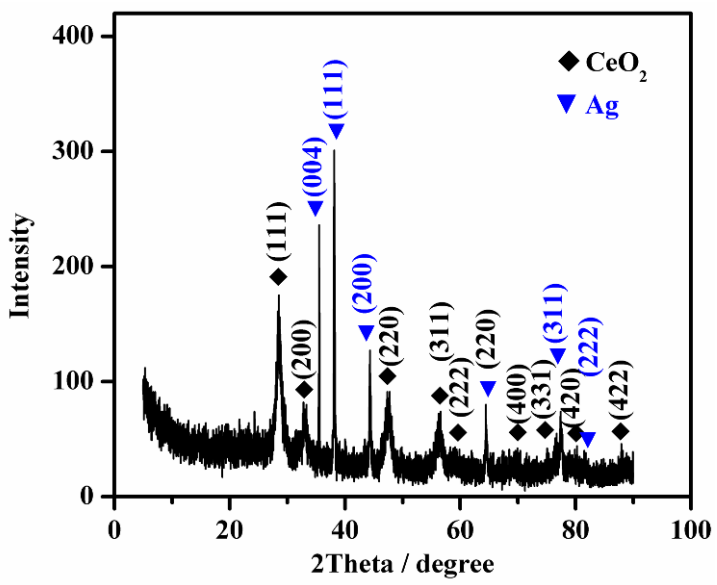

Fig. S20 XRD pattern of TSCeHSs after three cycles of photocatalytic reactions.

The formed Ag NPs are deposited onto the surface of the TSCeHSs during the photocatalytic process.

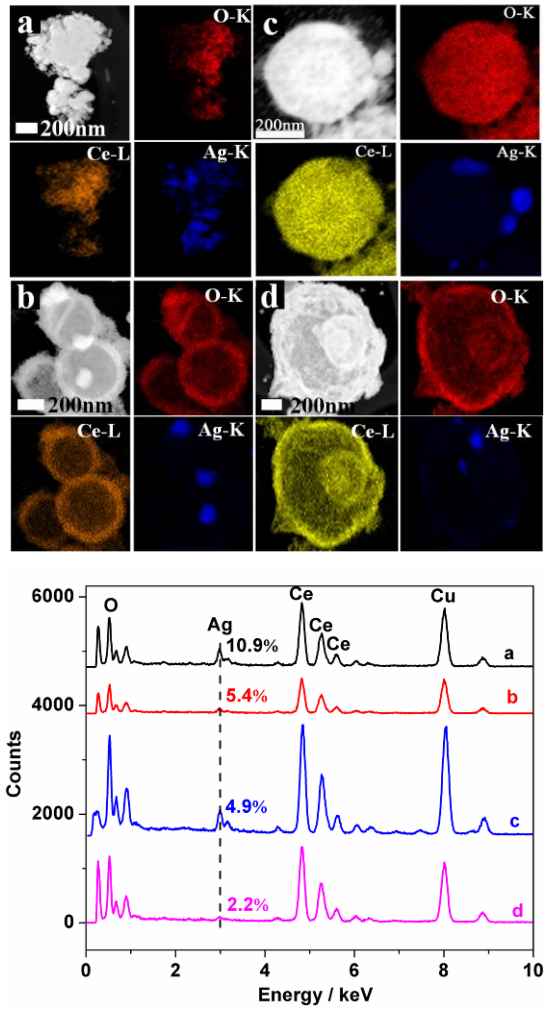

Fig. S21 HAADF-STEM mapping images (top) and corresponding EDX spectra (bottom) of four photocatalysts after three cycles of photocatalytic reactions. (a) commercial CeO_2 NPs, (b) SSCeHSs, (c) DSCeHSs and (d) TSCeHSs.

Elemental mapping by HAADF-STEM reveals that some Ag NPs are deposited on the surface of four photocatalysts, leading to the blockage of the active sites. EDX measurements indicate that the avergae amount of Ag NPs in the commercial CeO_2 NPs, SSCeHSs, DSCeHSs and TSCeHSs are 10.9%, 5.4%, 4.9% and 2.2%, respectively.

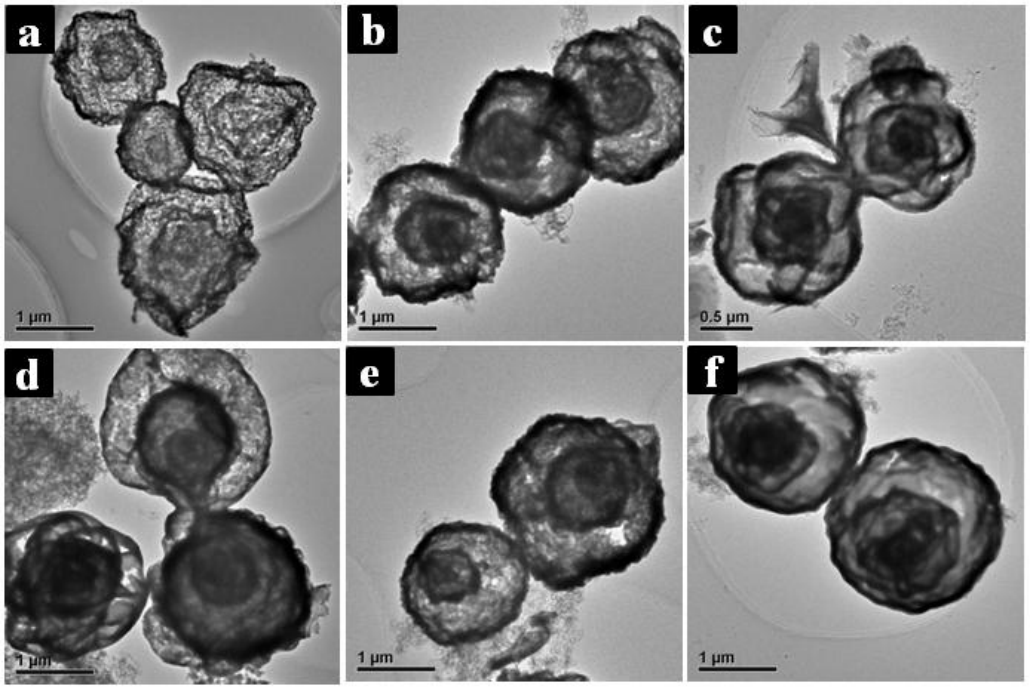

Fig. S22 TEM images of multi-shelled M_xO_y hollow microspheres in the mixed solution containing metal precursor, glucose and urea at 160 °C for 20 h: (a) Fe_2O_3, (b) CoO, (c) NiO, (d) CuO, (e) ZnO, and (f) CdO.

The general application of the "self-templating" approach is demonstrated, which can provide the solid foundation to construct other types of multi-shelled metal oxide hollow microspheres such as Fe_2O_3, CoO, NiO, CuO, ZnO, CdO and *etc.*

Table S1. BET surface area, average pore diameter, and total pore volume of commercial CeO_2 NPs, SSCeHSs, DSCeHSs and TSCeHSs.

Catalysts	BET surface area ($m^2\ g^{-1}$)	Average pore diameter (nm)	Total pore volume ($cm^3\ g^{-1}$)
CeO_2 NPs	5.1	1.9, 4.7	0.029
SSCeHSs	53.1	1.9, 8.3	0.097
DSCeHSs	55.8	3.6, 13.2	0.176
TSCeHSs	79.5	2.0, 8.5, 21.3	0.287

Surface areas and pore size distributions of the samples are calculated by using the Brunauer-Emmett-Teller (BET) equation and the Barrett-Joyner-Halenda (BJH) method, respectively.

Reference

1. L. Han, R. Liu, C. Li, H. Li, C. Li, G. Zhang and J. Yao, *J. Mater. Chem.*, 2012, **22**, 17079–17085.